Terahertz generation by GaAs nanowires

V. N. Trukhin, A. S. Buyskikh, N. A. Kaliteevskaya, A. D. Bourauleuv, L. L. Samoilov, Yu. B. Samsonenko, G. E. Cirlin, M. A. Kaliteevski, and A. J. Gallant

Citation: Appl. Phys. Lett. **103**, 072108 (2013); doi: 10.1063/1.4818719
View online: http://dx.doi.org/10.1063/1.4818719
View Table of Contents: http://aip.scitation.org/toc/apl/103/7
Published by the American Institute of Physics

Terahertz generation by GaAs nanowires

V. N. Trukhin,[1,2] A. S. Buyskikh,[1] N. A. Kaliteevskaya,[3] A. D. Bourauleuv,[1,3] L. L. Samoilov,[1,2] Yu. B. Samsonenko,[1] G. E. Cirlin,[1,3] M. A. Kaliteevski,[1,3] and A. J. Gallant[4]

[1]*Ioffe Physical Technical Institute, Russian Academy of Sciences, Polytechnicheskaya 26, 194021 St. Petersburg, Russia*
[2]*The National Research University of Information Technologies, Mechanics and Optics, 194000 St. Petersburg, Russia*
[3]*St. Petersburg Academic University - Nanotechnology Research and Education Centre, Russian Academy of Sciences, Khlopina 8/3, 194021 St. Petersburg, Russia*
[4]*School of Engineering and Computing Sciences, Durham University, Durham DH1 3LE, United Kingdom*

(Received 20 June 2013; accepted 28 July 2013; published online 13 August 2013)

We report on the emission of terahertz (THz) radiation from p-doped and intentionally undoped GaAs nanowires (NWs). The THz emission has been associated with the contributions of the drift and diffusion currents, excited in the 1D NWs. Taking into account the filling factor, the THz power emission for the NWs is shown to be 40 times more than that of the bulk epitaxial GaAs substrate. By analyzing the non-equilibrium dynamics of the photoinduced carriers in the nanowires, the charge carrier lifetime is shown to be of the order of 3 ns and the drift velocity 10^5 m/s. © *2013 AIP Publishing LLC*. [http://dx.doi.org/10.1063/1.4818719]

Over the past decade, THz radiation has been exploited in a wide variety of applications ranging from security scanners, subsurface non-destructive testing of materials to bio/chemical identification of explosives and drugs. However, compared to other regions of the electromagnetic spectrum, technical progress has been hindered by a shortage of readily available compact and powerful, coherent sources. One commonly used method to generate THz radiation is based on the illumination of a semiconductor substrate with a short (sub-picosecond) pulse of near infrared radiation. The THz radiation is induced either by non-linear optical rectification of the incoming pulse[1] or by excitation of a photocurrent.[2,3] The origin of the photocurrent can be attributed to: a surface or applied electric field (in which case, the THz generation is induced by drift current); ambipolar diffusion in inhomogeneous excitation (where the THz originates from diffusion currents); and anisotropy of the carrier distribution in momentum space which takes places at the interface between the semiconductor and a vacuum, in the simplest case.

In recent literature, it has been shown that the THz emission efficiency can be substantially increased if the bulk semiconductor is replaced with a structured surface. For example, emission from porous InP,[4] InN nanorods,[5] and ZnSe nanograins[6] has been reported as two orders of magnitude larger than their corresponding bulk samples. Likewise, silicon nanowires[7] and black silicon[8] have demonstrated much stronger emission than bare silicon wafers. InAs nanowires have about 15 times greater THz power efficiency than a planar InAs substrate.[9] The increase of THz generation efficiency with GaAs nanowires (NWs) was reported in our recent study.[10] It should also be mentioned that there is another type of quasi-one-dimensional structures, carbon nanotubes, in which strong slowing down of surface electromagnetic waves in single-wall carbon nanotubes and the ballistic electron motion may allow nanotubes to be used as nanoscale Cherenkov-type emitters in the terahertz frequency range.[11] This letter reports a detailed investigation of the mechanism behind the THz emission from these GaAs nanowires under short pulse illumination.

Three different NW samples were fabricated using an EP1203 MBE reactor, equipped with Ga, As, Be, and Au effusion cells. Each sample was grown by the so called "vapor-liquid-solid" (VLS) method, and all have a metal droplet on the top of the NW as shown in Figure 1. Sample F844 was grown in self-catalyzed mode and has Ga capping the top of NWs,[12] whereas samples F974 and F1032 were grown using a Au-catalyzed mode (see Figure 2). Detailed growth parameters and other properties of the samples are given in the supplementary material.[13]

To do so before the growth of sample F844, partial oxide desorption from the substrate surface was achieved by the thermal annealing 560 °C. After this stage, the substrate temperature was set to 590 °C, and the Ga shutter was opened briefly to allow liquid Ga droplets to form on the substrate surface in the pinholes of the oxide layer. The NW growth was performed in a Ga-stabilized growth regime using Be as a p-type doping impurity ($p = 1 \times 10^{18}$ cm^{-3}, as measured from a planar layer). The total growth time was

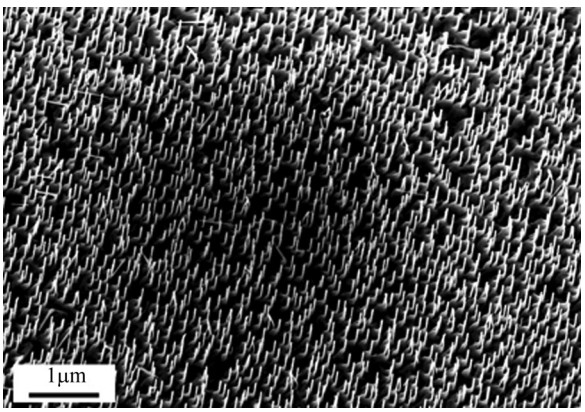

FIG. 1. SEM image of the sample F974.

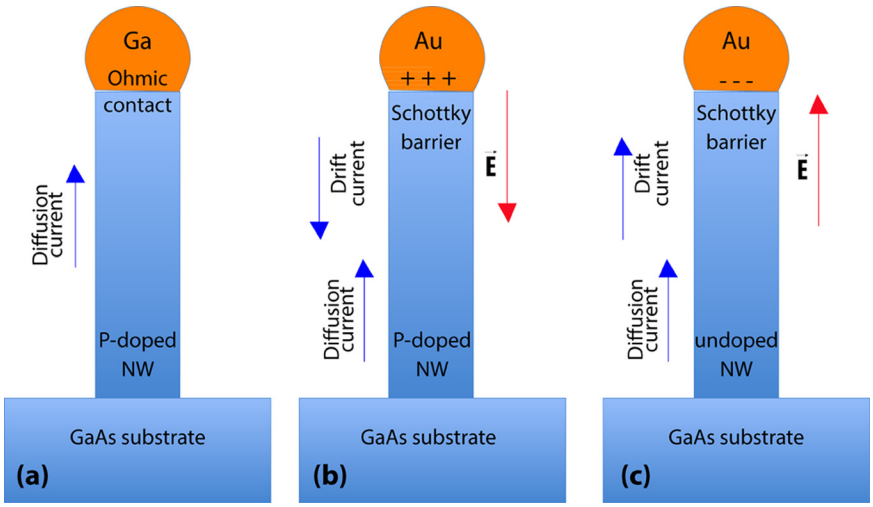

FIG. 2. The scheme of photocurrent in the sample under investigation. (a) p-doped nanowire with Ga cap, sample F844; (b) p-doped nanowire with Au cap, sample F1034; (c) n-doped nanowire with Au cap, sample F974.

15 min with a constant growth rate of 1 monolayer per second, resulting in ~1.2 μm long NWs with ~18 nm average diameter. When the growth was completed, a droplet of metallic Ga remained on the tip of the NWs. It is known that the GaAs-Ga contact under high temperatures, higher than 300 °C, changes to an ohmic contact (Mott-Curney contact[14,15]). In this case, no contact field exists at the Ga/GaAs interface as shown in Figure 2(a). Samples F974 and F1034 were grown by using Au as a growth catalyst, a 100 nm thick GaAs buffer layer was grown on the GaAs(111)B substrate for these samples after the total desorption of an oxide layer at 620 °C. The deposition of 0.3 nm thick Au layer was performed to promote the formation of NWs by the growth catalyst (at a temperature of 580 °C for F974 and 550 °C for F1034). Then NWs were grown at the same substrate temperatures. For sample F974, the NWs were undoped, but the NWs grown in such conditions could have slightly n-type doping with a concentration of the order 10^{16} cm^{-3}. Due to the relatively high substrate temperature, the NW height was much smaller (~300 nm), but the diameter was very similar to the sample F844 (~20 nm). The p-type GaAs(111)B substrate was used for the sample F1034 and the NWs were p-type doped as in the case of the sample F844. In the last case, the height and the diameter of the NWs were practically the same as for the first sample (height ~1 μm and diameter 20 nm). The Au/Ga droplet for samples F974 and F1034 leads to the formation of the Schottky barriers and therefore to the formation of an associated contact field, as shown in Figures 2(b) and 2(c). Note that the direction of the contact field depends on the type of doping of the NWs.

The growth of the samples was monitored using *in situ* Reflection High Energy Electron Diffraction (RHEED). All three samples were found to have a wurtzite crystallographic phase.

Photoexcitation of GaAs NWs was performed by Ti:Sapphire lasers operating at a wavelength of 800 nm with a repetition rate of 78 MHz, producing 10 nJ pulses with duration of 15 fs and 90 fs. In order to detect the THz emission, electro-optic sampling was used via a 1-mm thick ZnTe crystal. This provided electric field amplitude and phase information. For the power measurements, a Golay cell detector was used.

Experiments were conducted to determine the contribution of a nonlinear optical effect (also known as optical rectification): GaAs NWs were excited by femtosecond optical pulses, and the duration of the generated THz pulses was measured. If optical rectification is dominant in the emission, then the duration of the generated THz pulses should be comparable to that of the optical excitation pulse. Figure 3 shows the linear autocorrelation function for the sample illuminated by two consecutive 90-fs optical pulses. The power of the THz emission was measured in the specular direction as a function of the relative time delay between the pulses. It can be seen that the width of the autocorrelation peak is about 600f s, which is almost one order of magnitude greater than the optical excitation pulse length. Therefore, we can conclude that non-linear optical rectification (which is instantaneous) does not make a substantial contribution to the emitted THz power and instead photo-induced charge carriers dominate the generation mechanism.

Our next task was to determine the contribution of semiconductor wafer and wetting layer in the THz generation and make a comparison to the semiconductor nanowires. Therefore we have investigated polarization and angular dependence of THz emission and reflectivity of IR radiation. The polarization and the angular dependences were studied at low excitation levels, and the experiments were conducted in a mirror reflection geometry. Figure 4 shows the THz emission intensity as a function of the s- and p-polarized excitation pulse angle of incidence. It can be seen that the THz

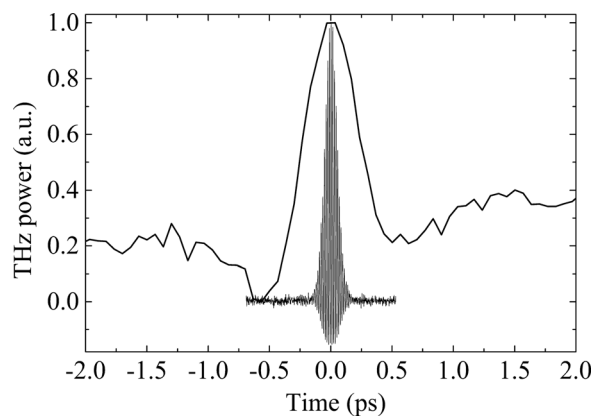

FIG. 3. Autocorrelation signal for a sample with GaAs NWs (solid line). Dotted line shows the intensity of optical excitation pulse.

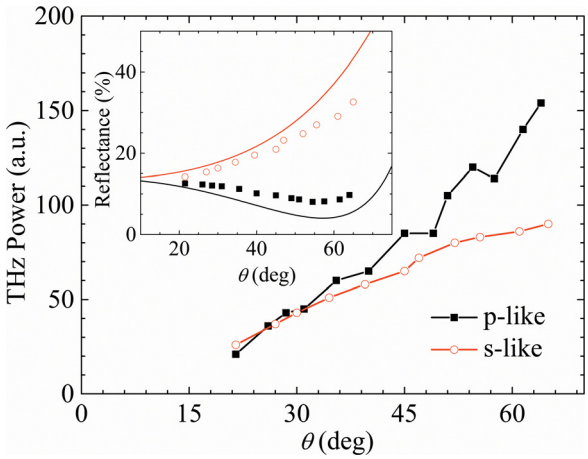

FIG. 4. Angular dependence of THz emission for s/p-polarizations. Inset: the angular dependence of reflectivity of the optical pump off the sample; solid lines are calculated dependencies.

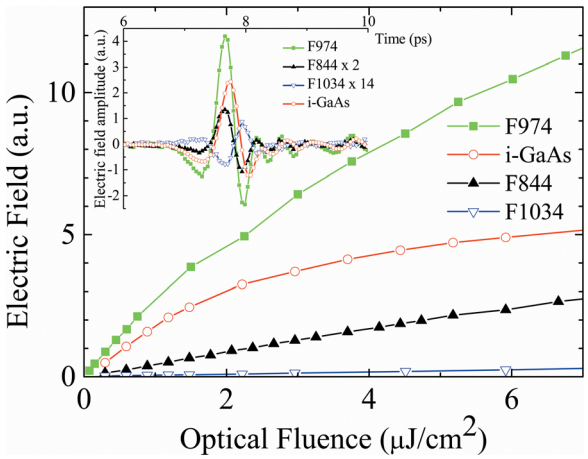

FIG. 5. Peak THz electric field E vs. F excitation density. Excitation pulses are p-polarized. Corresponding waveforms are given in the inset.

power monotonically increases with increasing angle for both polarizations. At an angle of 45°, the THz power for both polarizations is similar. This is in contrast to the emission characteristics of the bulk semiconductor surface which is shown in the inset of Figure 4 and is described with the well known Fresnel formula. Therefore the observed THz emission can be caused by the GaAs NWs mostly. Note also that, for the NW sample, the minimum value of the reflection coefficient was obtained at 57°, whereas for the bulk GaAs at 74°. Since the distance between the nanowires is of the order of 200 nm (see from Figure 1) the layer of NWs can be considered as a quasi-uniform media. Fitting of the reflectivity angular dependence allows an effective complex refractive index of $n_{\text{eff}} = 1.42 + 0.83i$ to be obtained. This corresponds to an absorption coefficient of 5 micron^{-1}, which is similar to that of bulk GaAs despite filling factor for NW layer being only about 1%.

Such high absorption in the NW layer can be attributed to the formation of a surface plasmon in the metallic droplets of the NWs. It can result in an electric field enhancement, which leads to increased absorption near the droplet (as shown in Figure 2(d)). Due to the higher mobility of electrons, the ambipolar diffusion of the electron-hole plasma from the top of the NW toward the substrate induces a pulse of photoexcited diffusion current from the substrate to the top of the NW, as illustrated in Figure 2. At the same time, the drift current can be caused by the movement of the photoinduced electron-hole plasma in the Schottky barrier contact field. The drift and diffusion currents can be parallel or anti-parallel depending on the NW doping type. Furthermore, due to the small filling factor, the effective refractive index for THz radiation is close to the unity, and the total internal reflection angle is greater than that of bulk GaAs. Hence, more THz radiation can leave the sample.

Several experiments were conducted to determine the specific mechanism which governs the emission of THz from GaAs nanowires. Waveforms of THz pulses from the NW samples and a bulk sample were recorded to determine dependence of THz electric field amplitude on the excitation intensity. Figure 5 shows the peak THz electric field amplitude for bulk epitaxial GaAs and for the NW samples F844, F974, and F1034. The THz waveforms are shown in the inset. It can be seen that the n-doped GaAs NWs with gold caps have the strongest THz response, exceeding those of bulk epitaxial GaAs. This confirms that GaAs NWs can be used for the fabrication of efficient THz emitters. It should be noted that the p-doped wires have a THz response that is weaker than that of the bulk sample. Such behavior can be explained using following arguments: The Ga cap forms an ohmic contact with NW, and there is no contact field (sample F844). Thus in this case there is a photoinduced diffusion current of the electrons and the holes from the top to the bottom of NW as shown in Figure 2(a). For the p-doped sample with an Au-droplet (sample F1034), there is a Schottky barrier contact field which is directed toward the substrate. The optical excitation pulse induces an ambipolar diffusion current of the electrons and the holes from the droplet and a drift current toward substrate. The drift and diffusion currents are contra directional, and in this case, the THz response is the weakest. For this sample, the maximum amplitude of the electric field of the waveform has the opposite sign compared to the same value for samples F974 and F844 (see the inset in Figure 5).

In contrast, for n-doped NWs, with an Au droplet, the diffusion current from the substrate to droplet is co-directional to the drift current, and the efficiency of THz emission is the highest. It should be mentioned that for low excitation powers, the dependence of THz field vs excitation is linear, and after a certain threshold it becomes sub-linear, as shown in Figure 5. It is worth noting that the length of the linear portion for F974 is much shorter than for F844. It can be explained by the strong surface field present in F974 which is negligibly small in F844. It is known that the movement of nonequilibrium electrons and holes in the surface field causes screening of this field and, subsequently, lowers the efficiency of THz generation. This dynamic screening of the surface field by nonequilibrium electrons and holes leads to the sub-linear dependency of the THz pulse electric field amplitude on the excitation intensity. As there is no contact field in F844, the dynamic screening due to the separating electrons and holes also does not exist, and this sub-linear dependency will be defined by the absorption coefficient saturation in the 1D semiconductor structure, and its saturation threshold will differ.

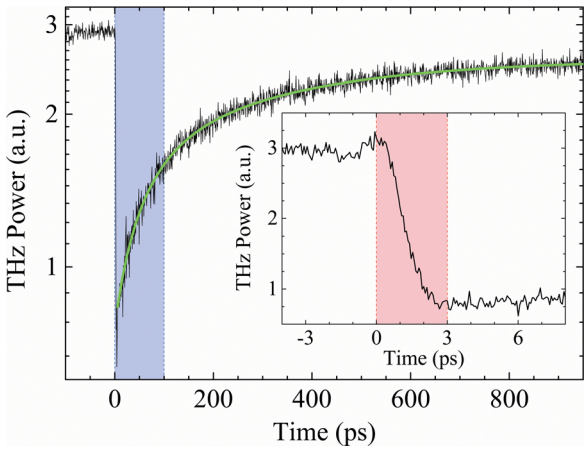

FIG. 6. The measured THz energy as a function of time delay relative to the prepulse for n-type GaAs NW. The inset shows this dependence for a small delay value.

An additional proof of dynamic screening in F974 was derived from the analysis of the nonequilibrium charge carriers' transport. Understanding the dynamics of charge carriers in semiconductor nanostructures is critical to the use of these materials in electronic and optoelectronic devices. To investigate these dynamics we have used two continual optical pulses to excite the photo-induced charge carriers in the NWs and investigate the dependence of THz power on the pulse time delay. The pulse intensities were chosen to ensure a linear THz response to excitation. Both the first and the second excitation pulses have a duration of 90 fs. However, the sequence of the "second pulses" was additionally modulated, and detection of THz radiation was synchronized with modulation of the "second pulse." Thus, the influence of the carriers created by the first optical pulse on THz emission from the carriers created by the second optical pulse moving in the NWs was investigated.

It should be noted that the diameter of the semiconductor NWs obtained, d, is less than or equal to 20 nm. The Bohr radius of the exciton, a_{ex}, in GaAs is 14 nm.[16] As long as $d < 2a_{ex}$, the nature of the electronic states is affected by quantum confinement. Therefore, such nanostructures can exhibit 1D transport properties even at room temperature.

Figure 6 shows the time dynamics of THz radiation from the moment when electron-hole plasma was excited by the "first optical" pulse. The maximum suppression of THz power takes place when the delay between optical pulses is 3 ps. This can be explained by the separation of photoinduced carriers in the contact field with subsequent screening of the contact field. As Schottky barrier depletion region has a length of about 1 micron,[17] assuming that the contact field is spreading on the length of the nanowires (300 nm), one can estimate the drift velocity of carriers as 10^5 m/s.

Subsequent restoration of THz power is due to charge trapping, recharging capacity of the Schottky barrier, and the carrier recombination that occurs in two stages. The first stage of this restoration is fast, mainly due to the charge trapping, recharging capacity of the Schottky barrier, and appears only at a high first pulse optical intensity and high carrier density, whereas further recovery of THz power is mainly associated with nonsaturable carrier recombination. The duration of the first stage is about 72 ps in the case considered. At low intensity of the first optical pulse, the first stage is absent, and there is slow recovery of THz power with a time in the course of 3 ns.

It should be mentioned that, in the case of charge trapping at the NW's surface and low intensity of the first optical pulse, the initial deep decay of THz generation would not be observed, and the following restoration would be fast. Nonradiative recombination due to charge trapping at the NW's surface reduces the charge carrier lifetime in GaAs NWs to 1 ps.[18] Therefore, charge carrier dynamics observed in our experiments is explained by carrier transport in the 1D NW structure.

In conclusion, we measured the THz emission from GaAs NWs induced by drift and diffusion photocurrents. The contribution of the drift current is greater than the contribution of the diffusion current in GaAs NWs with an Au/Ga droplet on their tips. THz emission from GaAs NWs can be 40 times higher than that from the bulk epitaxial GaAs surface taking into account the fill factor. Additional excitation of NWs by IR pulses leads to a steep drop in the THz power followed by slow monotonic recovery up to the prior level.

The study was supported by The Ministry of Education and Science of Russian Federation (Project No. 14.B37.21.1617), the RFBR, and the EU FP7 IRSES POLATER program.

[1]S. L. Chuang, S. Schmitt-Rink, B. I. Greene, P. N. Saeta, and A. F. J. Levi, Phys. Rev. Lett. **68**, 102 (1992).
[2]X.-C. Zhang, J. T. Darrow, B. B. Hu, D. H. Auston, M. T. Schmidt, P. Tham, and E. S. Yang, Appl. Phys. Lett. **56**, 2228 (1990).
[3]J. E. Pedersen, I. Balslev, J. M. Hvam, and S. R. Keiding, Appl. Phys. Lett. **61**, 1372 (1992).
[4]M. Reid, I. V. Cravetchi, R. Fedosejevs, I. M. Tiginyanu, and L. Sirbu, Appl. Phys. Lett. **86**, 021904 (2005).
[5]H. Ahn, Y.-P. Ku, Y.-C. Wang, C.-H. Chuang, S. Gwo, and C.-L. Pan, Appl. Phys. Lett. **91**, 132108 (2007).
[6]S. He, X. Chen, X. Wu, G. Wang, and F. Zhao, J. Lightwave Technol. **26**, 1519 (2008).
[7]G. B. Jung, Y. J. Cho, Y. Myung, H. S. Kim, Y. S. Seo, J. Park, and C. Kang, Opt. Express **18**, 16353 (2010).
[8]P. Hoyer, M. Theuer, R. Beigang, and E.-B. Kley, Appl. Phys. Lett. **93**, 091106 (2008).
[9]D. V. Seletskiy, M. P. Hasselbeck, J. G. Cederberg, A. Katzenmeyer, M. E. Toimil-Molares, F. Léonard, A. A. Talin, and M. Sheik-Bahae, Phys. Rev. B **84**, 115421 (2011).
[10]V. N. Trukhin, A. S. Buyskih, A. D. Buravlev, G. E. Cirlin, D. P. Horkov, L. L. Samoilov, and Y. B. Samsonenko, in *Proceedings of the 37th International Conference on Infrared, Millimeter, and Terahertz Waves, Wollongong*, Australia, 23–28 September 2012.
[11]K. G. Batrakov, O. V. Kibis, P. P. Kuzhir, M. R. da Costa, and M. E. Portnoi, J. Nanophotonics **4**, 041665 (2010).
[12]G. E. Cirlin, V. G. Dubrovskii, Yu. B. Samsonenko, A. D. Bouravleuv, K. Durose, Y. Y. Proskuryakov, B. Mendes, L. Bowen, M. A. Kaliteevski, R. A. Abram, and D. Zeze, Phys. Rev. B **82**, 035302 (2010).
[13]See supplementary material at http://dx.doi.org/10.1063/1.4818719 for detailed growth parameters and properties of the samples.
[14]Y. A. Goldberg, M. V. Ilina, E. A. Posse, and B. V. Tsarenkov, Sov. Phys. Semicond. **22**(3), 342 (1988).
[15]V. L. Berkovits, T. V. Lvova, and R. V. Khasieva, Sov. Phys. Semicond. **24**(6), 650 (1990).
[16]S. O. Kognovitskii, V. V. Travnikov, Ya. Aaviksoo, and I. Reimand, Phys. Solid State **39**, 907 (1997).
[17]M. B. Johnston, D. M. Whittaker, A. Corchia, A. G. Davies, and E. H. Linfield, Phys. Rev. B **65**, 165301 (2002).
[18]P. Parkinson, J. Lloyd-Hughes, Q. Gao, H. H. Tan, C. Jagadish, M. B. Johnston, and L. M. Herz, Nano Lett. **7**, 2162 (2007).